



Cranfield

College of Aeronautics Report No 9107
July 1991

A linearised Riemann solver for the time-dependent Euler equations of gas dynamics

E.F.Toro

Department Aerodynamics and Fluid Mechanics
College of Aeronautics
Cranfield Institute of Technology
Cranfield, Bedford MK43 0AL, England



Cranfield

College of Aeronautics Report No 9107
July 1991

A linearised Reimann solver for the time-dependent Euler equations of gas
dynamics

E.F.Toro

Department Aerodynamics and Fluid Mechanics
College of Aeronautics
Cranfield Institute of Technology
Cranfield, Bedford MK43 0AL. England

ISBN 1 871564 30 1

£8.00

*"The views expressed herein are those of the author alone and do not
necessarily represent those of the Institute"*

A LINEARISED RIEMANN SOLVER FOR THE TIME-DEPENDENT EULER EQUATIONS OF GAS DYNAMICS.

by

E F Toro

Department of Aerodynamics and Fluid Mechanics
College of Aeronautics
Cranfield Institute of Technology
Cranfield, Beds. MK43 0AL, England

ABSTRACT

The time-dependent Euler equations of Gas Dynamics are a set of non-linear hyperbolic conservation laws that admit discontinuous solutions (e.g. shocks). In this paper we are concerned with Riemann-problem based numerical methods for solving the general initial-value problem for these equations.

We present an approximate, linearised Riemann solver for the time-dependent Euler equations. The solution is direct and involves few and simple arithmetic operations. The Riemann solver is then used, locally, in conjunction with the WAF numerical method to solve the time-dependent Euler equations in one and two space dimensions with general initial data. For flows with shocks waves of moderate strength the computed results are very accurate. For severe flow regimes we advocate the use of the present linearised Riemann solver in combination with the exact Riemann solver in an adaptive fashion. Numerical experiments demonstrate that such an approach can be very successful. One and two-dimensional test problems show that the linearised Riemann solver is used in over 99 % of the flow field producing net computing savings by a factor of about 2. A reliable and simple switching criterion is also presented. Results show that the adaptive approach effectively provides the resolution and robustness of the exact Riemann solver at the computing cost of the simple linearised Riemann solver. The relevance of the present methods concerns the numerical solution of multi-dimensional problems accurately and economically.

to appear in PROC. ROY. SOC. LONDON (Sept. 1991)

1. INTRODUCTION.

Riemann-problem based methods (or RP methods) have made a significant impact in Computational Fluid Dynamics in the last decade. Their initial success for compressible, time-dependent inviscid flows with shock waves has been extended to other hyperbolic flows such as steady supersonic flows, shallow water flows and more recently, to parabolic flows such as the compressible Navier Stokes equations.

Key characteristics of RP methods is their ability to capture shock waves and other sharp features with optimal resolution and without the spurious oscillations (or much reduced) of traditional finite difference methods with added artificial viscosity. Their conservative character ensures correct positions of the computed shock waves and their robustness is a much appreciated feature, particularly in an industrial computing environment.

Despite their computational attractions, RP methods are more complex than traditional methods. Also, they are three to four times more expensive in computing time. The introduction of linearised Riemann solvers (e.g. Roe, 1981, 1986) meant a significant step forward in terms of simplification of algorithms and reduction of computing expense. As a result, however, accuracy and robustness for some special but important flow regimes has been compromised. Examples are very strong shocks, low-density flows (Einfeldt et al, 1991) and shear waves.

In this paper we present another approximate Riemann solver based on a local linearisation of the Euler equations. The solution is direct and involves few and very simple arithmetic operations. The Riemann solver is then used in conjunction with the Weighted Average Flux (or WAF, for short) numerical method (Toro, 1989b) to solve the time-dependent, non-linear Euler equations. For flows containing shock waves of moderate strength, that is pressure ratios of about three, the numerical results are very accurate. For severe flow regimes we advocate the adaptive use of the present Riemann solver in conjunction with the exact Riemann solver in a single numerical method. The WAF method offers the necessary flexibility to do this, as it uses the exact solution of the Riemann problem or any approximation to it. To this end we also propose a simple and reliable switching criterion with little empiricism.

Tests on a very severe blast-wave problem, where the initial data for pressure differs by five orders of magnitude, show that the linearised Riemann solver is used to solve 99.8 % of all Riemann problems in the computations; the quality of the solution is identical to that obtained when using the exact Riemann solver throughout. We are thus effectively obtaining the accuracy and robustness of the exact Riemann solver at the expense of the simplest Riemann solver.

The rest of this paper is organized as follows: In section 2, after recalling the main features of the exact solution of the Riemann problem, we present the linearised Riemann solver and a switching criterion. In section 3 we assess the performance of the linearised Riemann solver. Conclusions are drawn in section 4.

2. A LINEARISED RIEMANN SOLVER.

The Riemann problem for the time-dependent, one-dimensional Euler equations is the initial-value problem with piece-wise constant data ρ_L, u_L, p_L and ρ_R, u_R, p_R . The left (L) and right (R) states are separated by a discontinuity at $x=0$. The solution is self-similar and contains four constant states separated by three waves as shown in the $x-t$ picture of Fig. 1. The left and right waves are usually called acoustic waves, as they are associated with the eigenvalues $u-a$ and $u+a$ of the Jacobian matrix, where a is the sound speed. These waves can either be shock or rarefaction waves. The middle wave is always a contact discontinuity. There are therefore four possible wave patterns. Across the acoustic waves all variables change. The change takes place continuously across rarefactions and discontinuously across shocks. We call the region between the acoustic waves the *star region*. The pressure p^* and velocity u^* are constant throughout the star region, while the density jumps discontinuously from its constant value ρ_L^* to the left of the contact to its constant value ρ_R^* to the right of the contact.

No closed-form solution to the Riemann problem is known, not even for the case of ideal gases. Iteratively, however one can find the solution to any desired accuracy. Current exact Riemann solvers are based on solving a single non-linear algebraic equations for the pressure p^* (e.g. Toro, 1989a, 1991).

We now present a linearised approximate solution for the values in the star region. The one-dimensional, ideal time-dependent Euler equations are written in primitive-variable form as

$$\begin{bmatrix} \rho \\ u \\ p \end{bmatrix}_t + \begin{bmatrix} u & \rho & 0 \\ 0 & u & 1/\rho \\ 0 & \rho a^2 & u \end{bmatrix} \begin{bmatrix} \rho \\ u \\ p \end{bmatrix}_x = \begin{bmatrix} 0 \\ 0 \\ 0 \end{bmatrix} \quad (1)$$

or

$$W_t + AW_x = 0 \quad (2)$$

with the obvious notation for the vector of unknowns W and the coefficient matrix A . The components of W are density (ρ), pressure (p) and velocity (u); $a = \sqrt{\gamma p/\rho}$ is the speed of sound and γ is the ratio of specific heats. The coefficient matrix A depends on the solution vector W which makes system (2) non-linear. We perform a local linearisation as follows:

For sufficiently close nearby states W_L and W_R we assume the coefficient matrix A is constant and can be expressed in terms of an average state \bar{W} . This state is to be defined in terms of the data states W_L and W_R . Equations (2) become a linear system. The eigenvalues of A are

$$\lambda_1 = \bar{u} - \bar{a}, \quad \lambda_2 = \bar{u}, \quad \lambda_3 = \bar{u} + \bar{a} \quad (3)$$

with associated right eigenvectors

$$R_1 = \begin{bmatrix} \bar{\rho} \\ -\bar{a} \\ \bar{\rho} \bar{a}^{-2} \end{bmatrix}, \quad R_2 = \begin{bmatrix} \bar{\rho} \\ 0 \\ 0 \end{bmatrix}, \quad R_3 = \begin{bmatrix} \bar{\rho} \\ \bar{a} \\ \bar{\rho} \bar{a}^{-2} \end{bmatrix} \quad (4)$$

Results (3)-(4) hold for the nonlinear case too, but here eigenvalues and eigenvectors are expressed in terms of the average state \bar{W} , yet to be defined.

In solving the Riemann problem we want to find values for p^* , u^* , ρ_L^* and ρ_R^* (see Fig. 1). This is accomplished by using standard techniques for linear hyperbolic systems. Across the left wave associated with the eigenvalue $\lambda_1 = \bar{u} - \bar{a}$ the jumps in ρ , u and p satisfy

$$\frac{d\rho}{\bar{\rho}} = \frac{du}{-\bar{a}} = \frac{dp}{\bar{\rho}\bar{a}}$$

giving the relations

$$\left. \begin{aligned} u + \frac{\bar{a}}{\bar{\rho}} &= \text{constant} \\ u + \frac{1}{\bar{\rho} \bar{a}} p &= \text{constant} \end{aligned} \right\} \quad (5)$$

Similar arguments applied to the wave families associated with eigenvalues $\lambda_2 = \bar{u}$, $\lambda_3 = \bar{u} + \bar{a}$ give

$$\left. \begin{aligned} u &= \text{constant} \\ p &= \text{constant} \end{aligned} \right\} \quad (6)$$

across the contact wave and

$$\left. \begin{aligned} u - \frac{\bar{a}}{\bar{\rho}} \rho &= \text{constant} \\ u - \frac{1}{\bar{\rho} \bar{a}} p &= \text{constant} \end{aligned} \right\} \quad (7)$$

across the right acoustic wave.

Relations (6) across the contact wave simply confirm the constancy of p^* and u^* in the star region, which is a property of the exact Riemann solver (see Fig. 1).

Application of (5) across the left acoustic wave gives

$$u_L + \frac{\bar{a}}{\bar{\rho}} \rho_L = u^* + \frac{\bar{a}}{\bar{\rho}} \rho_L^* \quad (8)$$

$$u_L + \frac{1}{\bar{\rho} \bar{a}} p_L = u^* + \frac{1}{\bar{\rho} \bar{a}} p^* \quad (9)$$

and of (7) across the right acoustic waves gives

$$u_R - \frac{\bar{a}}{\bar{\rho}} \rho_R = u^* - \frac{\bar{a}}{\bar{\rho}} \rho_R^* \quad (10)$$

$$u_R - \frac{1}{\bar{\rho} \bar{a}} p_R = u^* - \frac{1}{\bar{\rho} \bar{a}} p^* \quad (11)$$

As for the average values $\bar{\rho}$, \bar{a} there are several possible options. Two obvious choices are

$$\left. \begin{aligned} \bar{\rho} &= \frac{1}{2}(\rho_L + \rho_R) \\ \bar{a} &= \frac{1}{2}(a_L + a_R) \end{aligned} \right\} \quad (12)$$

$$\left. \begin{aligned} \bar{\rho} &= (\rho_L \rho_R)^{1/2} \\ \bar{a} &= \frac{1}{2}(a_L + a_R) \end{aligned} \right\} \quad (13)$$

The geometric mean for the density has two interesting connections. One relates to the Riemann problem for the isothermal gas dynamics equations, for which, if one assumes that both acoustic waves are rarefaction waves, an exact solution for the density in the star region exists and is given by

$$\bar{\rho} = (\rho_L \rho_R)^{1/2} \exp[-(u_R - u_L)/(2a)]$$

where a is a constant sound speed. The second connection is that to Roe's linearised Riemann solver (Roe, 1981), the Roe average for the density is precisely a geometric mean.

Another possible choice comes from considering the Riemann problem for the isentropic gas dynamics equations. These form a non-linear two by two system with a constant region star between the acoustic waves. Under the assumption that these two waves are rarefaction waves one can obtain a direct solution for ρ and a given as

$$\left. \begin{aligned} \bar{a} &= \frac{1}{2} (a_L + a_R) - \frac{1}{4} (\gamma-1)(u_R - u_L) \\ \bar{\rho} &= \rho_L \left(\frac{\bar{a}}{a_L} \right)^{2/(\gamma-1)} \end{aligned} \right\} \quad (14)$$

Choice (13) appears to be a good compromise between simplicity and accuracy, particularly when our intentions are to use the linearised Riemann solver only in regions of slowly-varying data. One could also select the frozen values to satisfy certain desired properties for the linearised Riemann solver, such as recognition of shocks or rarefactions.

Having chosen the average avalues equations (8)-(11) give the explicit solution

$$u^* = \frac{1}{2} (u_L + u_R) - \frac{(p_R - p_L)}{2\bar{\rho} \bar{a}} \quad (15)$$

$$p^* = \frac{1}{2} (p_L + p_R) - \frac{\bar{\rho} \bar{a}}{2} (u_R - u_L) \quad (16)$$

$$\rho_L^* = \rho_L + (u_L - u^*) \frac{\bar{\rho}}{\bar{a}} \quad (17)$$

$$\rho_R^* = \rho_R + \frac{\bar{\rho}}{\bar{a}} (u^* - u_R) \quad (18)$$

Note that for the case of an isolated contact discontinuity travelling with speed $u^* = u_L = u_R$ the solution (15) - (18) is exact. For numerical purposes this is a welcome property of the present approximate Riemann solver; capturing contacts is more difficult than capturing shock waves

We wish to use this Riemann solver only in regions of slowly varying data. First we set

$$\left. \begin{aligned} p_{\min} &= \min \{p_L, p_R\} \\ p_{\max} &= \max \{p_L, p_R\} \\ Q &= p_{\max} / p_{\min} \end{aligned} \right\} \quad (19)$$

and restrict the use of the linearised Riemann solver (15) - (18) to cases in which

$$p_{\min} \leq p^* \leq p_{\max} \quad (20)$$

This restriction forbids the case in which both acoustic waves are rarefactions (p^* is less than p_{\min}) and also the case of two shocks (p^* is greater than p_{\max}). The first case can lead to negative densities in the linearised solver; this is known to happen in all linearised Riemann solvers (Einfeldt et. al 1991). The second case leads to pressure ratios greater than Q , which exceeds the pre-chosen allowable ratio. Both the two-rarefaction and the two-shock cases arise naturally at reflective boundaries; it would be unwise to compromise accuracy and robustness in those regions.

From equation (16)

$$p^* = \frac{1}{2} p_{\min} (1 + Q) - \frac{\bar{\rho} \bar{a}}{2} (u_R - u_L)$$

which, if substituted into (19) gives

$$p_{\min} \leq \frac{1}{2} p_{\min} (1 + Q) - \frac{\bar{\rho} \bar{a}}{2} (u_R - u_L) \leq p_{\max}$$

Some manipulations produce

$$-p_{\min} (Q-1) \leq \bar{\rho} \bar{a} (u_L - u_R) \leq p_{\min} (Q-1) \quad (21)$$

Thus restrictions (20) on the pressure produce restrictions (21) on the velocity difference.

Some empiricism is still present when selecting Q in (19) and (21). A cautious and yet successful choice is $Q = 2$.

The extension of the linearisation to computing solutions to the two or three dimensional Euler equations is straightforward, as in the fractional-step procedure only the dimensionally-split Riemann problem needs be considered. For the two-dimensional Euler equations the x-split Riemann problem has variables p , ρ , u (normal component of velocity) and v (tangential component of velocity). The structure of Riemann problem is identical to that of the one-dimensional case shown in Fig. 1. In fact the solution for p , u and ρ is the same as in (15)-(18) and the solution for the velocity component v is v_L to the left of the contact wave and v_R to the right of the contact wave. Note that this is precisely as in the exact solution to the x-split Riemann problem.

As it stands, the linearised Riemann solver can compute entropy-violating solutions under locally sonic flow conditions. This problem is easily remedied by replacing the star state closest to the t-axis (see Fig. 1) by the solution along the t-axis obtained by using the exact equations with the value for pressure in the region star taken from the linearised Riemann solver.

3. TEST PROBLEMS.

Two kinds of tests are used to assess the accuracy of the proposed linearised Riemann solver. First we consider the local values in the star region and compare the approximate values to the exact solution. Then we assess the performance of the linearised Riemann solver when used, locally, to compute the global solution to the non-linear Euler equations. The local values are used to compute intercell numerical fluxes and then it is the flux difference that really matters in the solution updating procedure of conservative RP methods. In the author's experience appreciable errors in the local values are permissible before they begin to show in the numerical results, as we shall see.

3.1 LOCAL VALUES.

We consider the Riemann problem with data $\rho_L = p_L = 1.0$, $\rho_R = p_R = 1/2$ and $\gamma = 1.4$. We allow the velocities (and thus the velocity difference) to vary and consider three cases.

Table 1 shows a comparison of the present method with that due to Roe (Roe, 1981) and the exact solution.

| CASE A | | | | |
|---------|--------|--------|------------|------------|
| | p^* | u^* | ρ_L^* | ρ_R^* |
| PRESENT | 1.0 | 0.5 | 1.0 | 0.8571 |
| ROE | 0.8400 | 0.5482 | 0.9747 | 0.8881 |
| EXACT | 0.9689 | 0.5267 | 0.9777 | 0.7953 |

| CASE B | | | | |
|---------|--------|--------|------------|------------|
| | p^* | u^* | ρ_L^* | ρ_R^* |
| PRESENT | 0.7500 | 0.7817 | 0.8214 | 0.6786 |
| ROE | 0.6108 | 0.8061 | 0.7904 | 0.7096 |
| EXACT | 0.7009 | 0.7929 | 0.7758 | 0.6357 |

| CASE C | | | | |
|---------|--------|--------|------------|------------|
| | p^* | u^* | ρ_L^* | ρ_R^* |
| PRESENT | 0.5000 | 1.0634 | 0.6429 | 0.5000 |
| ROE | 0.4033 | 1.0751 | 0.6119 | 0.5257 |
| EXACT | 0.4982 | 1.0604 | 0.6080 | 0.4987 |

TABLE 1. Comparison of results for local values.

For case (a) the velocity difference takes the minimum value in inequality (21), in case (b) this difference is zero and for case (c) it takes the maximum value in inequality (21). The Roe values are obtained by re-interpreting Roe's Riemann solver as suggested by Toro (1991). It should be pointed out that Roe's numerical method does not use the star values of the solution of the local Riemann problem. It is legitimate however to use the Roe averages, corresponding wave strengths and right eigenvectors to compute the jumps in the conserved variables across the waves in the solution of the Riemann problem. In this way we can obtain values for p , u and ρ in the star region, and we call them the Roe values.

For the pressure and velocity values the present approximate Riemann solver is consistently more accurate than the re-interpretation of Roe's solver. For the density values the two approximate solutions are comparable. This test is very reassuring. Even more so when we do not propose to use the present approximate Riemann solver everywhere in the flow field but only at those places satisfying inequalities (2) for $Q = 2$, say.

3.2. NUMERICAL APPLICATIONS.

Here we use the Riemann-problem solution (15)-(18) locally, to compute intercell numerical fluxes as done in the Weighted Average Flux (WAF) method proposed by Toro (1989b). An updated version of the method as applied to the Euler equations is given by Toro (1991).

We consider four test problems. The first is a shock-tube test problem for which the pressures and densities are in the ratio 2 to 1. These are chosen as in section 3.1 with initial discontinuity at $x = 0.5$. For the velocities we take $u_L = u_R = 0$. This problem has exact solution and we use it to assess the performance of the approximations.

Fig. 2 shows a comparison between the numerical solution using the linearised Riemann solver throughout (symbol) and the exact solution (line) at time $t = 0.3$ units. The numerical solution is remarkably good for this test in which conditions (21) with $Q = 2$ are satisfied throughout. Choice (12) for the average values $\bar{\rho}$ and \bar{a} is used. In order to appreciate the quality of the solution for this reasonably mild test we solve the same problem using the two-step Lax-Wendroff method without artificial viscosity. Fig. 3 shows the results. In practice of course one uses the Lax-Wendroff method with artificial viscosity; this reduces the amplitude of the oscillations but smears discontinuities. This test clearly shows that even in the flow regions of slowly varying data we need to use sophisticated numerical methods such as RP methods.

The second test problem is the so called Sod's shock-tube test problem (Sod, 1978). It consists of a shock tube of unit length with diaphragm placed at $x = 1/2$ and left (L) and right (R) data given as

$$\begin{array}{lll} \rho_L = 1.0 & u_L = 0.0 & p_L = 1.0 \\ \rho_R = 0.125 & u_R = 0.0 & p_R = 0.1 \\ \gamma = 1.4 & & \end{array}$$

Fig. 4 shows a comparison between the computed (symbol) and exact (line) solutions at time 0.25 units. The linearised Riemann solver with average values (13) is used throughout. The quality of the solution is the same as that in which the exact Riemann solver is used throughout; see Fig. 5. This is encouraging, since for this test problem the initial pressure ratio is 10 and

the shock wave that results has pressure ratio 3. If average values (12) are used the computed solution is similar but slightly inaccurate near the tail of the rarefaction wave. Compare to the results of Fig. 6 obtained when Roe's method is used

As a third test for the method in which the linearised Riemann solver is used adaptively in conjunction with the exact Riemann solver we take the so called blast-wave test of Woodward and Colella (1984). It was specially designed to test both the robustness and accuracy of numerical methods. It is a severe test. This problem is also a shock-tube problem but has no exact solution. The main features of the solution are however well known and we expect our methods to reproduce those features accurately. The exact Riemann solver used is that given by Toro (1991).

A domain of unit length is discretised by $M = 3000$ cells and the initial shock-tube like data consists of three constant states separated by diaphragms at $x = 0.1$ and $x = 0.9$. The left (L), middle (M) and right (R) states are

$$\begin{array}{lll}
 \rho_L = 1.0 & \rho_M = 1.0 & \rho_R = 1.0 \\
 u_L = 0.0 & u_M = 0.0 & u_R = 0.0 \\
 p_L = 10^3 & p_M = 10^{-2} & p_R = 10^2 \\
 \gamma = 1.4 & &
 \end{array}$$

Fig. 7 shows the numerical results at time 0.028, shortly after the collision of the two strong shocks emanating from the initial discontinuities. The numerical solution was obtained with the adaptive Riemann solver with $Q = 2$. To plotting accuracy there is no difference between this solution and that obtained using the exact Riemann solver throughout.

The solution was evolved by 5185 time steps and more than fifteen and a half million local Riemann problems were solved out of which 99.8% were solved by the linearised Riemann solver (15) - (18).

As a fourth test problem we solved the two-dimensional, time-dependent Euler equations for flow over a wedge at an angle of 30 degrees to the oncoming stream. Fig. 8 shows the computational domain and the computed isopycnics at a fixed time. The flow travels from left to right at a Mach number of 5.5. The shock reflection pattern is known as double Mach reflection. To plotting accuracy this result is identical to that obtained when using the exact Riemann solver throughout. This two-dimensional computation was carried out by

Dr. James Quirk, to whom the author is indebted.

Finally, a CPU-time comparison is in order. For a typical problem the figures are: 1.0 for WAF with the linearised Riemann solver throughout; 1.03 for WAF using the linearised and exact Riemann solvers adaptively; 1.8 for Roe's method and 2.0 for WAF with the exact Riemann solver throughout.

5. CONCLUSIONS.

An approximate linearised Riemann solver applicable to the time-dependent Euler equations and a Riemann-problem adaptation procedure have been presented. For slowly-varying data the solver is sufficiently accurate to be used adaptively in conjunction with the exact Riemann solver. The practical usefulness of the proposed schemes is illustrated by solving realistic one and two-dimensional test problems. One of the most severe applications shows that the linearised Riemann solver is used to solve over 99 % of all Riemann problems solved in the computations without affecting the accuracy of the computed solution. Thus one effectively retains the accuracy and robustness of exact Riemann solvers at the computing cost of the very simple approximate Riemann solver presented in this paper.

REFERENCES.

1. Roe, P L, 1981.
Approximate Riemann solvers, parameter vectors and difference schemes. *Journal of Computational Physics*. 43, pp 357-372.
2. Roe, P L , 1986.
Characteristic-based schemes for the Euler equations. *Ann. Rev. Fluid Mech.* 18, pp 337-365.
3. Einfeldt, B., Munz C D, Roe P L and Sjögreen B. 1991.
On Godunov-type methods near low densities. *Journal of Computational Physics*, 92, pp 273-295.
4. Toro, E F, 1989a.
A fast Riemann solver with constant covolume applied to the Random Choice Method. *Int. J. Numer. Meth. in Fluids*, 9, pp 1145-1164.
5. Toro, E F, 1989b.
A weighted average flux method for hyperbolic conservation laws. *Proc. Roy. Soc. London, A* 423, pp 401-418.

6. Toro, E F, 1991.

The weighted average flux method applied to the Euler equations. In the press.

7. Woodward P and Colella P, 1984.

The numerical simulation of two-dimensional fluid flow with strong waves. Journal of Computational Physics, 54, pp 115-173.

8. Sod, G A, 1978

A survey of several finite difference methods for systems of non-linear hyperbolic conservation laws. Journal of Computational Physics, 27, pp 1-31

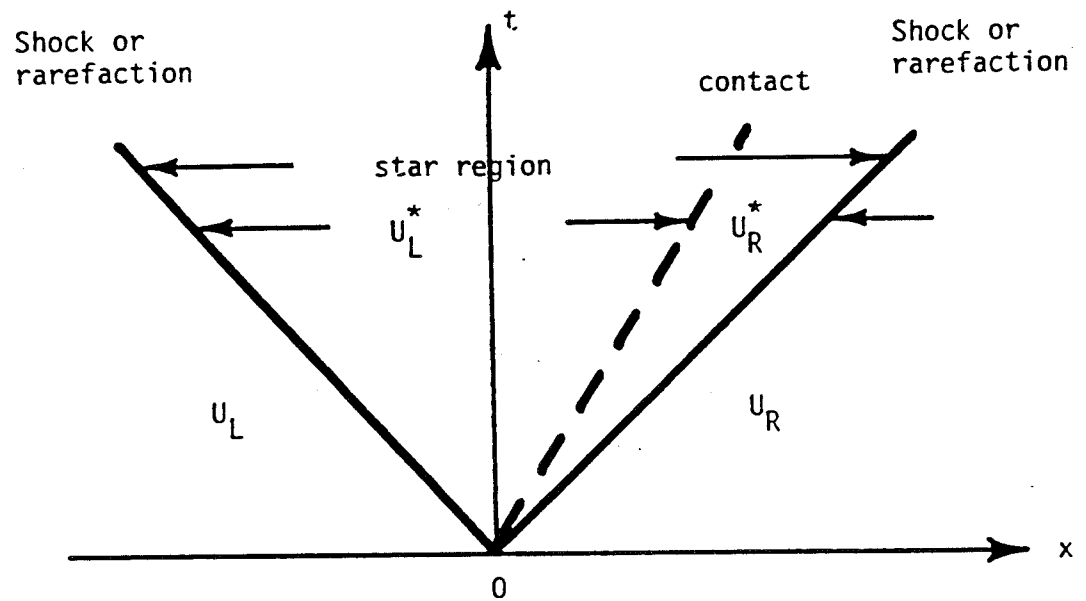


Fig. 1. Structure of the exact solution to the Riemann problem for the time-dependent, one-dimensional Euler equations. There are four constant states separated by three waves. Solution in region star between the left and right waves is main step to obtain complete solution.

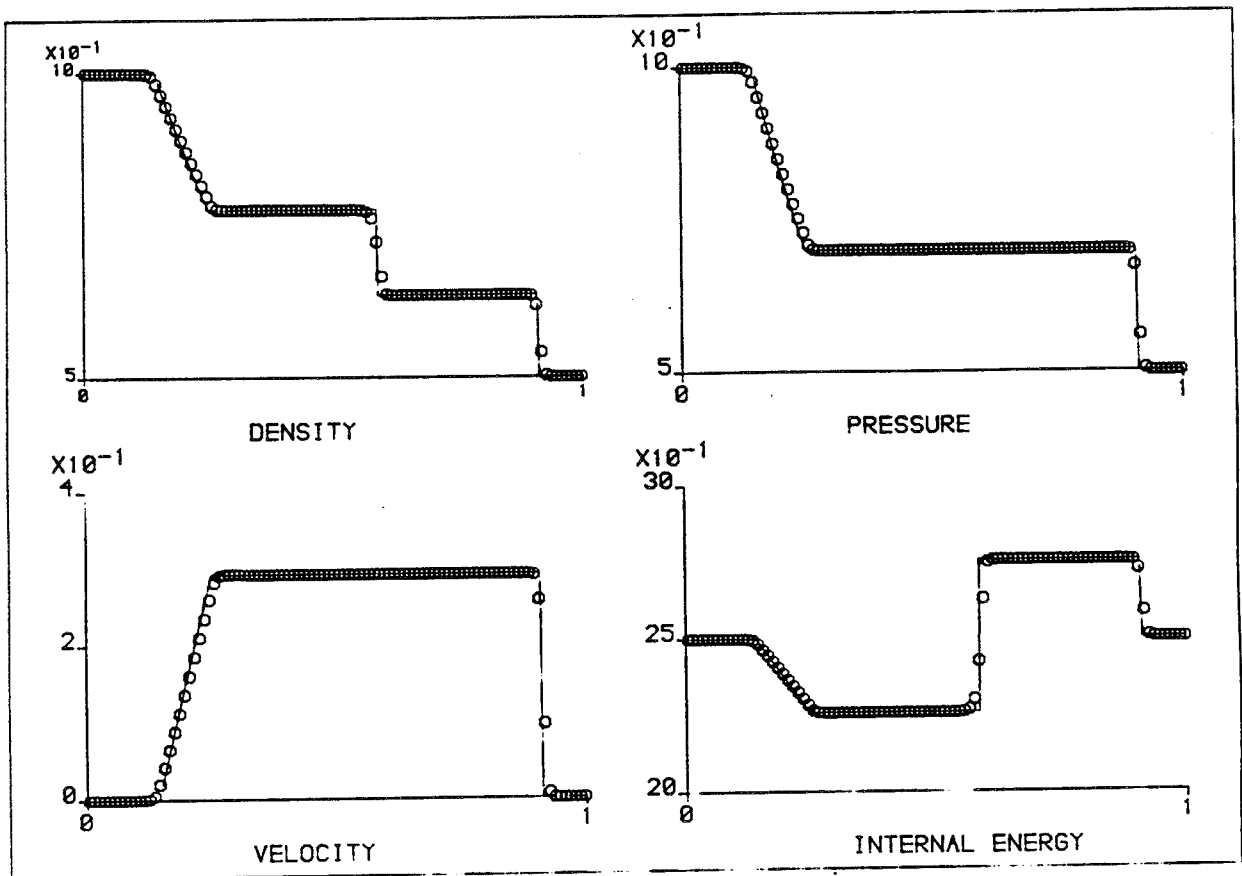


Fig. 2. Comparison between the numerical (symbol) and exact solutions for a shock-tube problem. The numerical solution was obtained with the WAF method using, locally, the present linearised Riemann solver throughout the flow field.

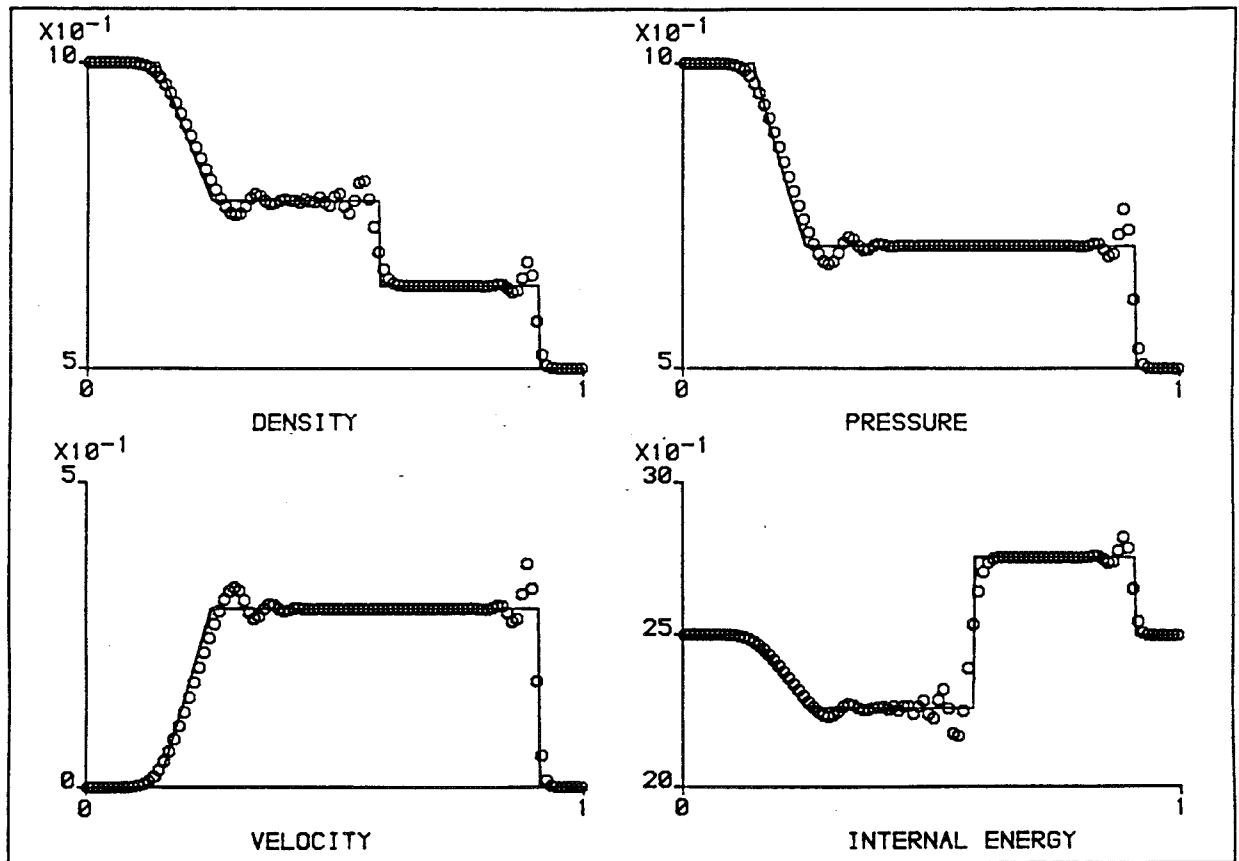


Fig. 3. Comparison between the numerical (symbol) and exact solution for a shock-tube problem. The numerical solution was obtained using the two-step Lax-Wendroff method without artificial viscosity.

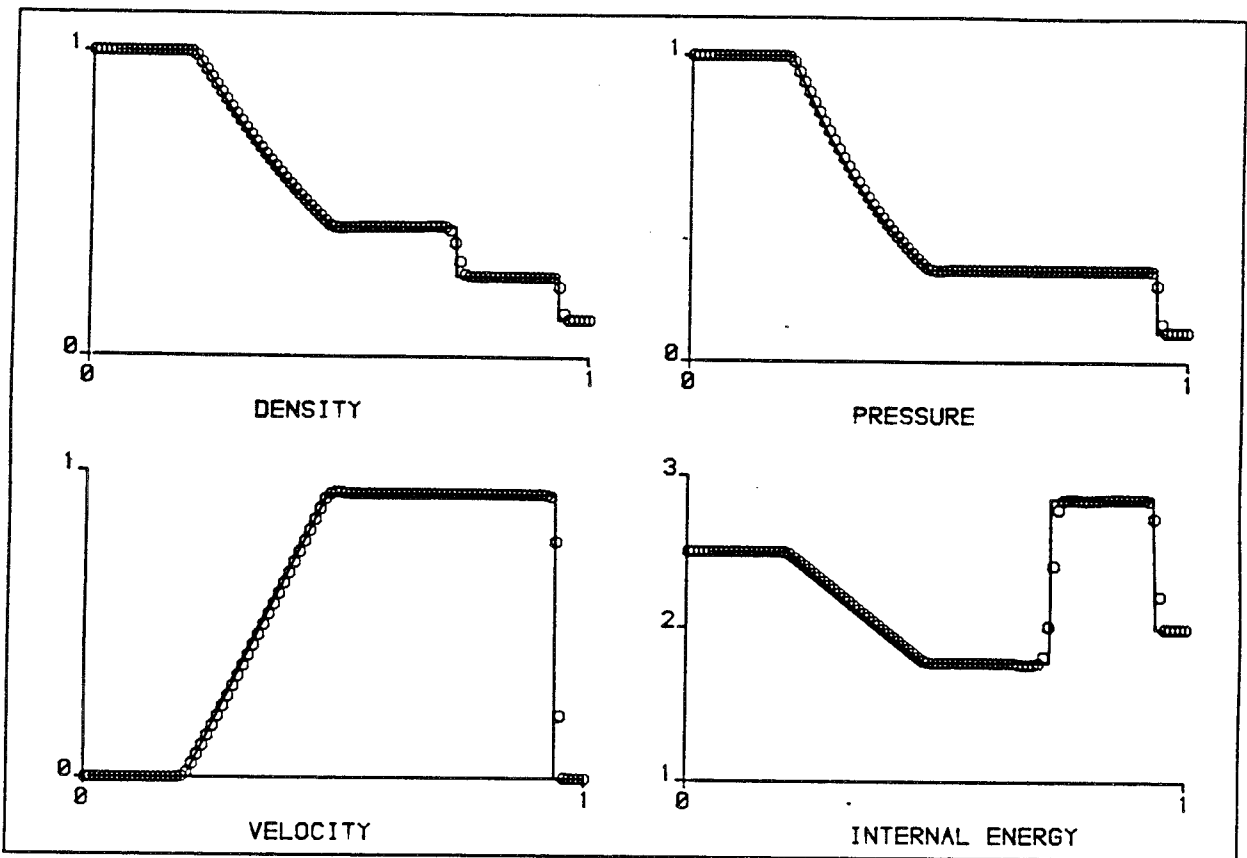


Fig. 4. Comparison between the WAF numerical (symbol) and exact (line) solutions to Sod's problem at time 0.25 units. The linearised Riemann solver is used throughout.

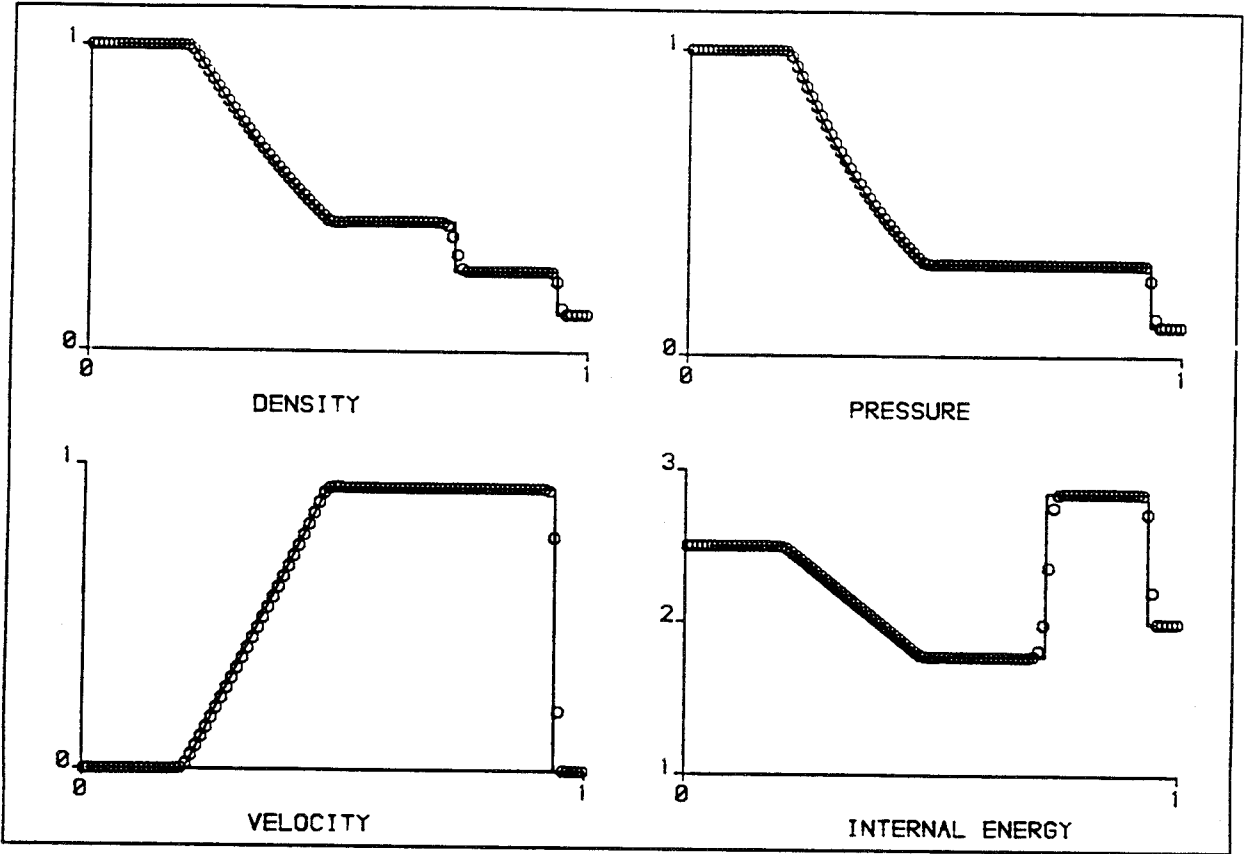


Fig.5 Comparison between the WAF numerical (symbol) and exact (line) solutions to Sod's problem at time 0.25 units. The exact Riemann solver is used throughout.

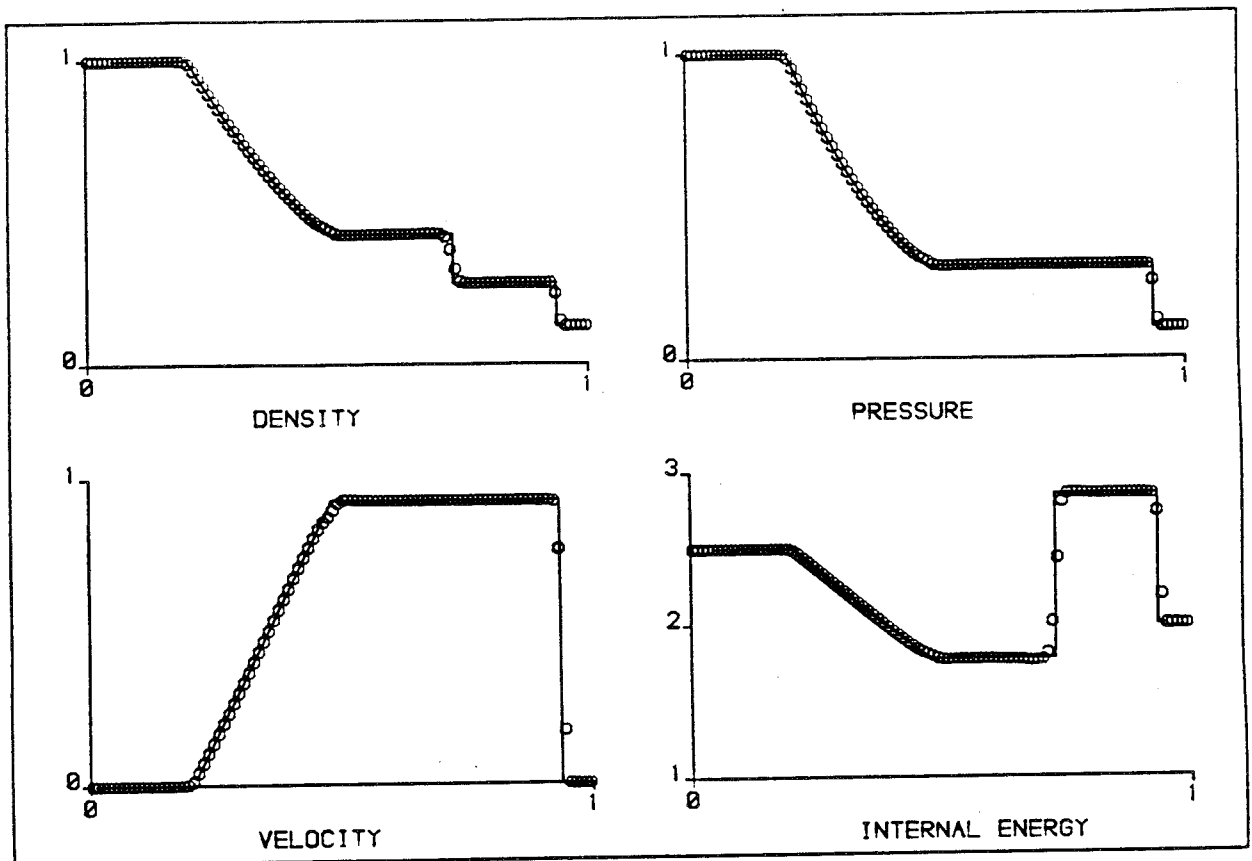


Fig. 6 Comparison between the Roe numerical (symbol) and exact (line) solutions to Sod's problem at time 0.25 units.

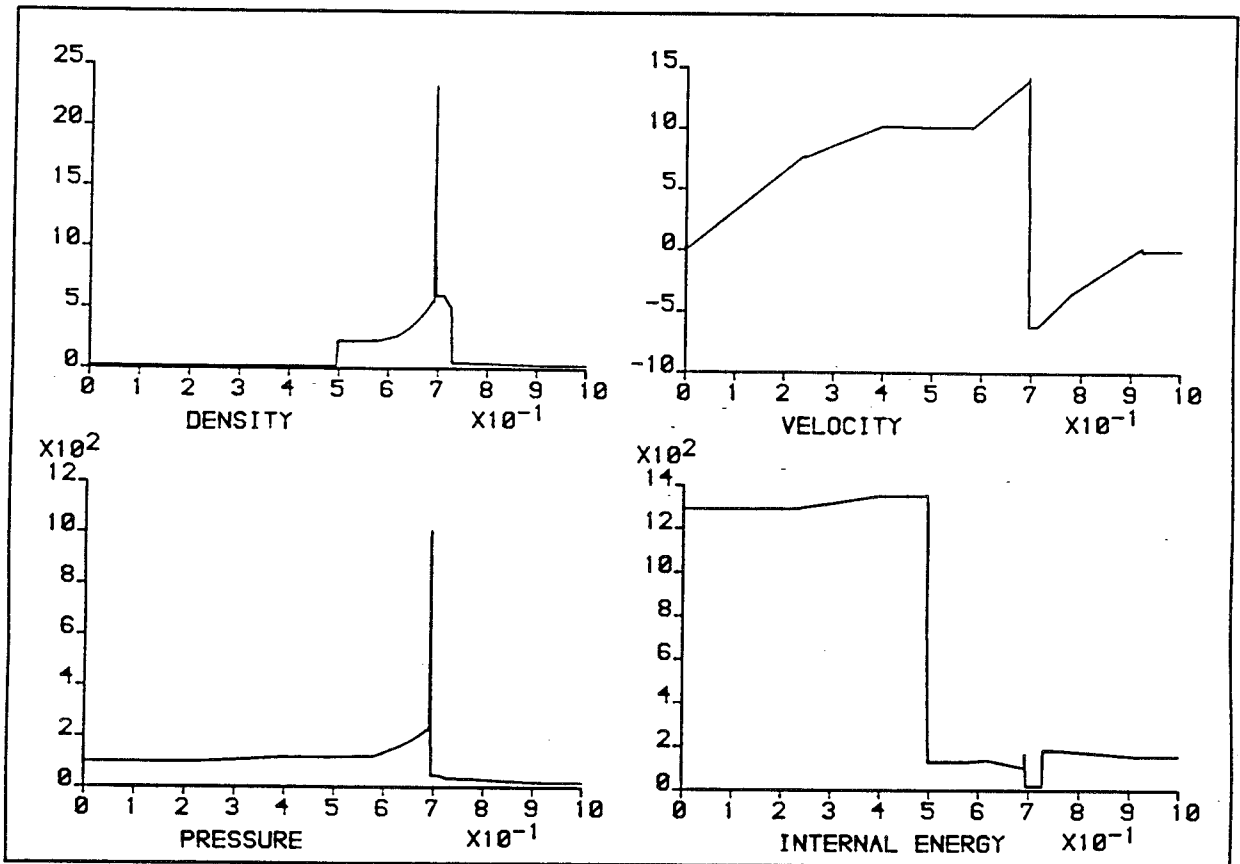


Fig. 7. Numerical solution (line and symbols) to the blast-wave problem of Woodward and Colella. The WAF method is used together with the linearised and the exact Riemann solvers used adaptively.

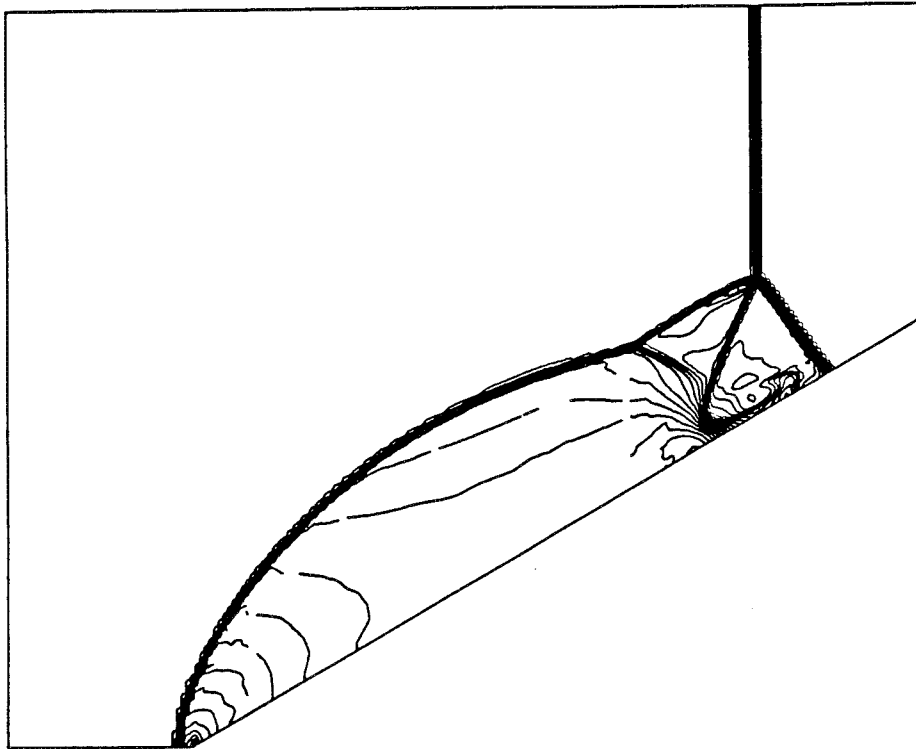


Fig. 8. Numerical solution of a double Mach reflection problem for flow at Mach 5.5 over a wedge at 30 degrees. The linearised and exact Riemann solvers are used adaptively.